# Design of Ablative Thrust Chambers and Their Materials

S. J. TICK,* G. R. HUSON,* AND R. GRIESE†
*Thiokol Chemical Corporation, Denville, N. J.*

**An analytical method of describing the ablation process using finite-difference techniques (Dusinberre) to compute multicomponent transient conduction and the effects of endothermic decomposition of the resin, including transpiration cooling and erosion of the char, has been validated by comparisons with data from firings of liquid rockets with silica phenolic chambers. The results may be used in design optimization and to establish goals for materials improvements. The thermal conductivity of the char layer and the density of the virgin silica phenolic material appear to be the strongest property variables affecting ablative performance. Doubling the thermal conductivity halves the erosion; halving the thermal conductivity increases chamber durability by a factor of 2. Doubling the virgin material density doubles both erosion resistance and time-to-char-through. However, increases in operating parameters (flame temperature and chamber pressure) produce much stronger effects on char depth and erosion rate than do materials properties.**

## Nomenclature

$A$ = area
$C_c$ = specific heat (char)
$C_v$ = specific heat (virgin)
$D$ = diameter
$\epsilon$ = emissivity
$\alpha_g$ = absorptivity
$F$ = shape factor
$f_v$ = volatile fraction
$f_r$ = resin fraction
$G$ = mass velocity
$H_d$ = heat of decomposition
$h$ = heat-transfer coefficient
$K_r$ = radiation constant
$k$ = thermal conductivity
$M$ = $\Delta r^2/\Delta\theta\alpha$
$M_g$ = molecular weight
$N$ = $\Delta rh/k$ Biot number
$P_c$ = chamber pressure
$Q$ = quantity of heat
$r$ = radius; $\Delta r$ = thickness increment
$R$ = $\Delta r_1\, k_2/\Delta r_2\, k_1$
$T$ = temperature
$T_d$ = decomposition temperature
$V$ = volume
$\dot{W}$ = weight flow rate
$\rho$ = density
$\sigma$ = Boltzmann constant
$\alpha$ = thermal diffusivity
$\Delta\theta$ = time increment

***Subscripts***

$d$ = decomposition
$g$ = gas
$c$ = char
$v$ = virgin

## Introduction

THE ablation of charring materials offers efficient thermal protection for liquid rocket thrust chambers, resulting in simpler lighter designs. Combustion heat is transferred to the wall, thus rapidly increasing the surface temperature. When the surface reaches a limiting temperature, a portion of the ablative material (usually the resin binder of a laminate) begins to decompose and absorbs a large part of the heat, thus preventing it from passing to the backup materials. The porous "char" layer that remains after this partial degradation has different thermophysical properties than the virgin material and functions as an insulator until eroded. Decomposition gases from the resin percolate through the char structure, cooling it, and finally pass into the combustion side boundary layer, reducing the heat-transfer coefficient. The char depth and the surface temperature continue to rise until at some characteristic surface temperature condition the char will be removed by a combination of mechanical shearing, chemical reaction, and melting.

The outstanding assets of successful ablative materials are their high sensible and latent heat capacities and their suitability for the creation in situ of high service temperature, low-density insulative char layers. Their liabilities include a definitely limited operational life, ending in catastrophic failure, and changes (often gross) of the gas-side contour and dimensions. The purpose of this paper is to present results obtained from an analytical study to determine the changes in physical and thermal properties of a silica phenolic ablator required to provide a profitable reduction in the erosion (surface regression) and charring of the ablative. Insights into the influence of the thermal properties of the virgin and char materials on performance thus obtained point out areas of potential improvement for specific applications. The equations used are solved by finite-difference techniques.[1] The method of attack involves multicomponent transient conduction and the concept of two moving boundaries. One boundary represents the decomposition of the resin, the evolution of gaseous products, and char formation; the second boundary represents the erosion of this char by high-temperature, high-velocity combustion gases.

## Finite-Difference Method

The physical model, an annular segment of unit length, is shown in Fig. 1. The chamber wall section considered is

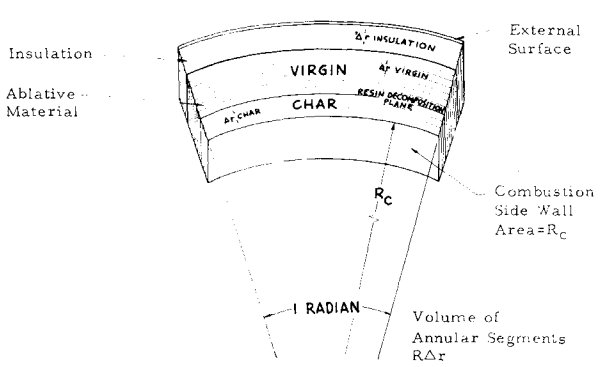


**Fig. 1 Model for segment of ablative thrust chamber wall.**

Presented as Preprint 64-261 at the 1st AIAA Annual Meeting, Washington, D. C., June 29–July 2, 1964; revision received November 2, 1964.

* Unit Supervisor, Thrust Chamber Section, Reaction Motors Division. Member AIAA.
† Programmer, Reaction Motors Division.

general in nature, consisting of an ablative material at the inner chamber wall, backed by any number of insulating or heat sink materials. The radius of this segment is divided into increments of $\Delta r$ thickness, and a "node" is considered to exist in each segment, providing reference points at which temperatures may be calculated. Starting from time zero, heat balances are taken at each nodal point in the cross section, and the temperature distribution for the segment is computed, based upon prior temperatures.[1] This process is repeated for increasing time until partial decomposition of the material and subsequently surface erosion require adjustments in the process.

Ablative materials are fabricated from high-temperature, fibrous reinforcement materials impregnated with organic resin binders. The binder resin is assumed to decompose completely at a constant temperature, requiring heat of decomposition ($\Delta H_d$). The transpiring decomposition gas is assumed to be in thermal equilibrium at each char node. While charring is in progress, the gas-side surface can erode at a rate related to surface temperature. The reduction of gas-side heat-transfer coefficient resulting from increased chamber diameter is considered; the addition of decomposition gases to the boundary layer is also considered. Thermal radiation interchange between chamber surfaces is also considered, including radiation to space through the nozzle exit.

A heat balance on a half-block at the inner surface, which considers radiation, convection, and conduction, yields the following equation for computing the gas-side surface temperature for an increment of time:

$$Q_{\text{in}} = Q_{\text{stored}} + Q_{\text{out}} \tag{1}$$

or

$$h_g r_n [T_g - T_n]\Delta\theta + \sigma(\epsilon_g T_g^4 - \alpha_g T_n^4) r_n \Delta\theta = (k A_n/\Delta r)\,(T_n - T_{n+1})\Delta\theta + \rho C_p V (T_n^1 - T_n) + \epsilon F \sigma r_n (T_n^4 - T_s^4)\Delta\theta \tag{2}$$

Equation (2) can be transformed into the form

$$T_n^1 = \frac{N_g r_n T_g + T_n\left[\frac{M}{2}\left(r_n + \frac{\Delta r}{4}\right) - N_g r_n - \left(r_n - \frac{\Delta r}{2}\right)\right] + \left(r_n + \frac{\Delta r}{2}\right) T_{n+1} + K_{SR}\,(T_n^4 - T_S^4) - K_{gr}(\epsilon T_a^4 - \alpha_c T_n^4)}{\frac{M}{2}\left(r_n + \frac{\Delta r}{4}\right)} \tag{3}$$

The derivation of the internal temperature equation for the same material is similar to that given previously for the surface equation; however, the radiation term is absent and heat transfer occurs by conduction only. A heat balance around an internal node ($n$) yields, for internal temperatures,

$$T_n^1 = \frac{[r_n - (\Delta r/2)]T_{n-1} + T_n[(M-2)r_n] + T_{n+1}[r_n + (\Delta r/2)]}{M_1 r_n} \tag{4}$$

A nodal point is made to occur at each material interface. In the following equations for the heat balance around such a nodal point, the subscript "$n$" refers to the nodal temperature; subscripts 1 and 2 refer to the adjacent materials:

$$T_n^1 = \frac{\left(r_n - \frac{\Delta r1}{2}\right) T_{n-1} + T_n\left[\frac{M_1}{2}\left(r_n - \frac{\Delta r_1}{4}\right) + \frac{M_2}{2}\left(\frac{\Delta r_1}{\Delta n_2}\frac{k_2}{k}\right)\left(r_n + \frac{\Delta r_2}{4}\right) - \left(r_n - \frac{\Delta r_1}{2}\right) - \frac{\Delta r_1}{\Delta n_2}\frac{k_2}{k_1}\left(r_n + \frac{\Delta r_2}{2}\right)\right] + \frac{\Delta r_1}{\Delta r_2}\frac{k_2}{k_1}\left(r_n + \frac{\Delta r_2}{2}\right) T_{n+1}}{\frac{M_1}{2}\left(r_n - \frac{\Delta r_1}{4}\right) + \frac{M_2}{2}\left(\frac{\Delta r_1}{\Delta r_2}\frac{k_2}{k_1}\right)\left(r_n + \frac{\Delta r_2}{4}\right)} \tag{5}$$

The temperature-time equation for the outside surface is similar to that derived for the internal surface [Eq. (3)]. The equation becomes

$$T_n^1 = \frac{T_{n+1}\left(r_n - \frac{\Delta r}{2}\right) + T_n\left[\frac{M}{2}\left(r_n - \frac{\Delta r_2}{4}\right) - N_0 r_n - \left(r_n - \frac{\Delta r}{2}\right)\right] - K_{r0} T_n^4 + N_0 r_n T_0}{\frac{M}{2}\left(r_n - \frac{\Delta r}{4}\right)} \tag{6}$$

The decomposition of the binder resin results in a discontinuity and must be considered as soon as the predicted temperature at a given node $T_n$ exceeds the decomposition temperature $T_d$. The decomposition temperature is assumed to be a constant to simplify the analysis. Rigorously, resin decomposition occurs over a temperature range that can be determined in the laboratory from a thermogravimetric analysis; however, in this analysis the temperature at which 50% of the total weight of volatile material in the test specimen has been volatilized is used. When $T_d$ is reached, the problem becomes the prediction of the advance of the char-virgin material interface. The heat potentially available for the decomposition of the resin ($q_d$) is obtained by first calculating the heat remaining for storage at the interface node. Not all of this heat is used for vaporizing the resin since some is used in raising the adjacent char and the virgin material temperatures. The remainder, however, is available for resin pyrolysis; thus,

$$Q_d = \Delta r_c \Delta H_d \rho_v [r_n + (\Delta r_c/2)] + \rho_v C_v \Delta r_c [r_n + (\Delta r_c/2)]\,(T_d - T_v) \tag{7}$$

As the resin pyrolyzes, the decomposition gases pass through the porous char, cooling its structure, as they flow toward the surface. Since the heat capacity of the gas flow is small compared to that of the char, and the heat-transfer coefficient and pore surface area are large, the gases are assumed to be in thermal equilibrium with each char nodal point. The gas flow changes the balance because of transpiration cooling, resulting in the following changes in Eqs. (3) and (4), respectively,

$$T_n^1 = \frac{\left(r_n - \frac{\Delta r_c}{2}\right) T_{n-1} + T_n\,[(M-2)r_n] - \frac{\dot{W}_{cg} C p_g \Delta r_c}{2k_c}\,(T_{n-1} - T_{n+1}) + \left[r_n + \frac{\Delta r_c}{2}\right] T_{n+1}}{M_c r_n} \tag{8}$$

$$T_n^1 = \frac{N_g r_n T_g + T_n\left[\frac{M_c}{2}\left(r_n + \frac{\Delta r_1}{4}\right) - N_g r_n - \left(r_n + \frac{\Delta r_1}{2}\right)\right] + \left[r_n + \frac{\Delta r_1}{2}\right] T_{n+1} - K_r(T_n^4 - T_S^4) - \frac{\dot{W}_{cg} C p_g \Delta r_c}{2K_c}\,(T_n - T_{n+1})}{\frac{M_1}{2}\left(r_n + \frac{\Delta r_1}{4}\right)} \tag{9}$$

The equation recommended by Hildalgo[2] is used to compute the reduction in heat-transfer coefficient caused by decomposition gases entering the boundary layer

$$\frac{h}{h_0} = \frac{C_p}{C_{p0}}\left[1 - \frac{1}{5}\left(\frac{M_g}{M_d}\right)^{\delta}\frac{\Delta r_c}{\Delta\theta}\,\rho_v f_r f_v C_{p0}\right] \qquad (10)$$

$$\delta = \tfrac{4}{5} \text{ if } M_g/M_d > 1$$

$$\delta = \tfrac{1}{3} \text{ if } M_g/M_d < 1$$

The erosion of the char is dependent upon many factors, among which are wall shear forces, viscosity of the melted char, heat of fusion and/or vaporization of the char, and reactions in the boundary layer. Since these mechanisms are not completely understood for all of the ablative materials, it was felt that the use of a rate equation as a function of surface temperature only would be more useful. Munson[3] states that, "for those materials which form a char layer, simultaneous measurements of recession rate and surface temperature suggest that the erosion rate is uniquely determined by the surface temperature." The equation that he suggested is

$$\dot{r} = K_1 T_{gc}^{K_2} \exp(-K_3/T_{gc}) \qquad (11)$$

where $K_1$, $K_2$, and $K_3$ are constants, and $T_{gc}$ is the gas-side char surface temperature. The constants $K_1$, $K_2$, and $K_3$ have been determined at Reaction Motor Division (RMD) for a number of materials in small-scale rocket motor firings. It is assumed that there is no heat loss or gain due to erosion of the material.

It is acknowledged that this approach to erosion is a simplification of the actual physical process. However, the goal of this analysis is to provide a working technique for the prediction of erosion in ablative materials, rather than a detailed analysis of the process associated with one particular ablative. The validity of this approach, however, has been demonstrated by comparisons with actual test data (even for solid propellants), as will be shown later.

The required input data fall into two basic categories: engine parameters and ablative material characteristics. The engine operating parameters are chamber pressure, flame temperature, characteristic velocity, combustion efficiency, throat area, transport properties of the combustion gases, number of insulation materials, structural wall thickness, external environment, and engine duty cycle. Duty cycles may be separated by long heat-soak periods. Heat soaks affect both the char depth and the erosion loss; when a rocket motor is shut down, the heat stored in the char material continues to generate char for a length of time dependent upon the length of the fire time and the storage capacity of the residual char. The flexibility of this computer program enables it to accept any type of duty cycle. The properties associated with the ablation material are often quite difficult to obtain; they include the decomposition temperature of the resin, heat of decomposition of resin, weight fraction of resin, weight fraction of resin that decomposes to gases, thermal conductivity of virgin material, density of virgin material, specific heat of virgin material, thermal conductivity of char, density of char, specific heat of char, molecular weight of resin decomposition gases, specific heat of decomposition gases, and empirically determined erosion constants. The properties of the char are usually unknown and must be either measured or computed approximately by the methods outlined in Refs. 4 and 5.

**Table 1 Base value of parameters**

| | | | |
|---|---|---|---|
| Operating parameters | | | |
| Initial $P_c$, psia | | 120 | |
| Throat area, in.$^2$ | | 19.6 | |
| Chamber diam, in. | | 7.05 | |
| Combustion performance, % | | 98.0 | |
| Theoretical $T_g$, °F | | 5200 | |
| Material properties | | | |
| | Silica phenolic | Insulation | Aluminum |
| Thickness, in. | 0.5 | 0.2 | 0.04 |
| $k$, Btu/hr-ft$^2$-°F/ft | 0.28 | 0.058 | 89.5 |
| $\rho$, lb/ft$^3$ | 108 | 47 | 173 |
| $C$, Btu/lb-°F | 0.3 | 0.35 | 0.23 |
| Silica phenolic ablative properties | | | |
| $T_d$, °F | | | 1000 |
| $\Delta H_d$, Btu/lb | | | 335 |
| Resin fraction, $f_r$ | | | 0.35 |
| Resin vapor fraction, $f_v$ | | | 1 |
| $C_d$ (decomposition gases), Btu/lb-°F | | | 0.3 |
| $M_d$ | | | 16 |
| $\rho_c$, lb/ft$^3$ | | | 69 |
| $k_c$, Btu/hr-ft$^2$-°F/ft | | | 0.28 |
| $C_c$, Btu/lb-°F | | | 0.3 |

## Discussion

This analytical program has been applied to both the determination of the most fruitful changes in ablative material properties and the scaling of thrust chambers. In regard to the former, variations in the physical properties of the ablative materials have been employed without regard to either the feasibility of their manufacture or to the recognized interrelationships between some of the physical and thermal properties of the materials. Efforts have been made to describe the ablative mechanisms in terms of physical properties that can or should be measurable in the laboratory by conventional analytical techniques. In regard to scaling factors, the influences of run parameters (such as chamber pressure, firing duration, wall thickness, flame temperature, and propellants) upon the performance of ablators in thrust chambers is investigated. In preliminary design activities and mission optimization studies, it is essential that the influence of these parameters upon ablator performance and the consequent weight of the thrust chamber is predictable.

### Approach

"Time-to-char-through" (the time at which the charring reaches the interface between the ablative and the backup insulator) has been chosen as the figure of merit in evaluating ablative performance. The relationship between time-to-char-through and thickness can be used to determine the chamber weight necessary for a given firing duration. Two cases are presented: with erosion and without erosion. Since state-of-the-art engines can utilize the techniques of mixture ratio shifts and slight chamber pressure reductions to avoid erosion completely, the nonerosive case was considered to be of greater interest. However, the identical case based on erosion starting at a surface temperature of 4300°F was evaluated for comparison. The erosion process is influenced only by the surface temperature, which is, in turn, determined by other processes and the property variables. Time-to-char-through is a sufficient description of the performance of ablators in most stations of the thrust chamber; however, if one proposes to utilize the ablator in the throat of the exit nozzle for the thrust chamber, the erosion loss becomes an important variable for design.

All of the erosion rates were calculated for a 100-sec firing; however, it is believed that conclusions relative to the influence of the various physical properties upon erosion are valid for longer durations as well. Table 1 shows the base values of the parameters used in this study.

## Results

The results of the analyses are presented in Figs. 2–7 as dependent variables plotted against relative changes in the

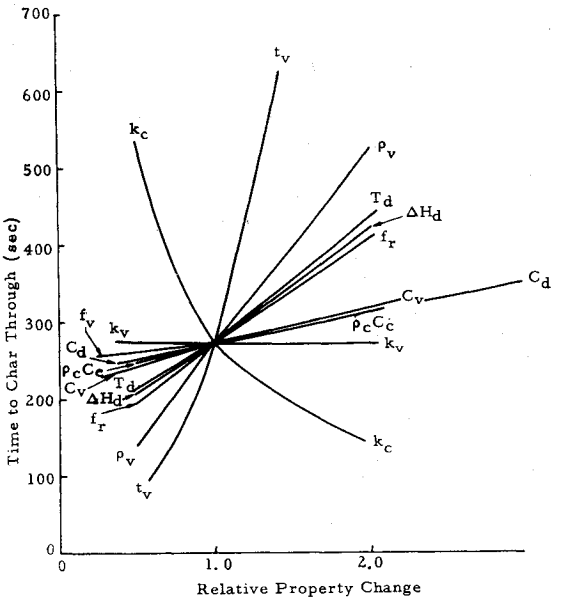


**Fig. 2 Time-to-char-through vs material property change (no erosion).**

independent variables. Figure 2 shows the influence of the physical and thermal properties of the ablative on the time-to-char-through without erosion. Figure 3 presents the same independent variables with time-to-char-through (considered with erosion) as the dependent variable. Figure 4 shows erosion rate in the first 100 sec of firing as a function of the material properties. The same figures of merit are plotted as functions of the run parameters in Figs. 5–7. The steeper the slope, the stronger the influence of the variable under consideration. It should be noted that ablative performance with erosion is less sensitive to the variables than without erosion. Erosion, therefore, results in a leveling effect, which implies that improvements in ablative materials will become increasingly difficult to obtain as erosion becomes the dominant process. In the following sections, the influence of the various properties and parameters will be discussed in approximate order of significance.

### Material Property Variables

Ablator thickness has the strongest influence upon performance in terms of time-to-char-through, with or without erosion (Figs. 2 and 3). The thicker the ablator, the longer it will take to char through because of the additional material; however, in the absence of erosion, additional ablative materials also results in additional insulation by the char. This accounts for the increasing slope shown in Fig. 2. With erosion, however, the relationship between time-to-char-through and thickness is simply linear over the range investigated, indicating that steady-state charring is occurring. The thickness has no influence upon erosion rate in the first 100 sec of firing (Fig. 4); this result is probably due to the low thermal conductivities of the char and the virgin material.

The density of the virgin material ($\rho_v$) influences the amount of sensible heat storage that occurs while the material is being heated to $T_d$. It also determines the heat of decomposition per unit volume of resin and the quantity of gas that percolates through the char. Furthermore, $\rho_v$ (along with $f_r$ and $f_v$) determines the char density and, thereby the sensible heat of the char. Therefore, increasing the $\rho_v$ is beneficial to performance in terms of both time-to-char-through and erosion rate (Figs. 2–4). It should be pointed out, however, that greater gains in time-to-char-through can be achieved by thickening the materials, rather than by increasing $\rho_v$; e.g., doubling $\rho_v$ has the same benefit as thickening the material by 30–50% (Fig. 2). However, low-density ablators usually do not exhibit good erosion resistance and cannot be utilized where erosion losses are intolerable. The lightest composite chamber wall for a given duration would have a primary ablator (with maximum erosion resistance) of a thickness exactly equal to the erosion loss, backed up by a low-density material with the best possible charring properties. In the throat of a thrust chamber, where specific impulse losses due to erosion must be traded off against weight, increased $\rho_v$ results in reduced erosion.

The thermal conductivity of the char material is inversely related to chamber durability, both with and without erosion, since the char material functions as an insulator formed in place by the resin decomposition process. However, higher conductivities remove heat from the eroding surface rapidly, reducing the surface temperature and decreasing the erosion rate. Without erosion, the influence of the char insulation on time-to-char-through is extremely important, but erosion reduces this effect appreciably (compare Figs. 2 and 3).

The latent heat of decomposition ($\Delta H_d$) represents a very large portion of the total heat sink capability of the ablative. Chamber durability with and without erosion and the erosion rate are improved significantly by increasing $\Delta H_d$, which serves to reduce the erosion rate by reducing surface temperature and postponing the attainment of the erosion temperature.

When the fraction of resin ($f_r$) was evaluated as a variable, $\Delta H_d$ was also changed, since in this analysis $\Delta H_d$ is a

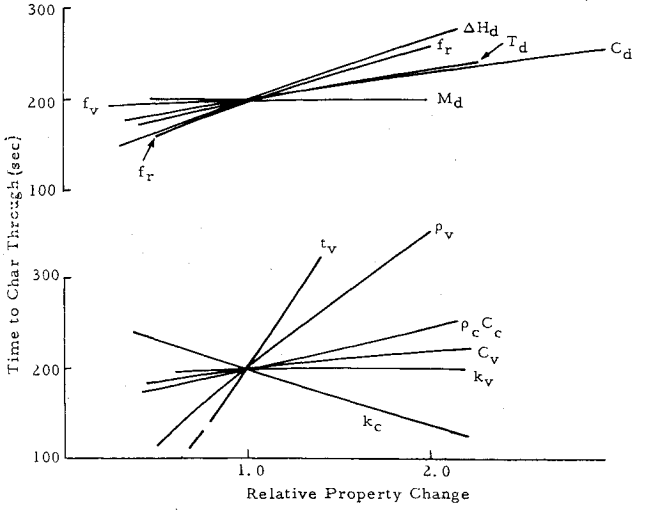


**Fig. 3 Time-to-char-through vs material property change (with erosion).**

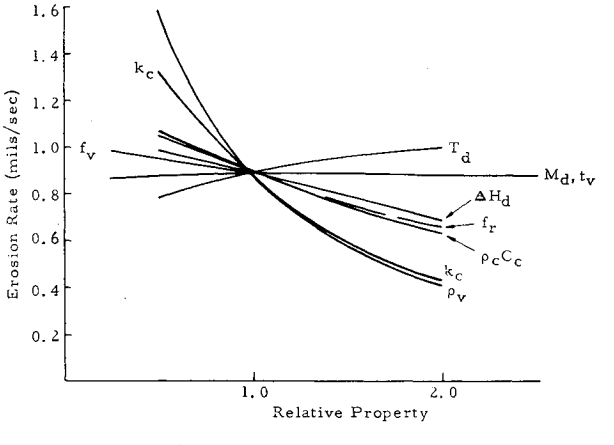


**Fig. 4 Thermophysical property influence on erosion.**

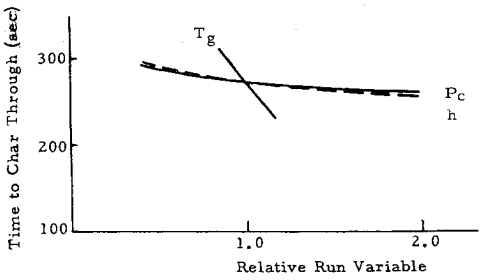


**Fig. 5 Time-to-char-through with run variable changes (no erosion).**

dependent variable. It may be seen that the results for both these variables ($\Delta H_d, f_r$) are quite similar. Resin fraction influences all of the physical properties of the virgin material and the char thermal properties as well as the char's structural properties. However, these latter influences have not been considered in this analysis (except for influence on char density).

The resin decomposition temperature ($T_d$) ranks with $\Delta H_d$ and $f_r$ in favorably influencing durability for the nonerosion case (Fig. 2), but it is much less effective when erosion occurs (Fig. 3). The curve of erosion rate (Fig. 4) shows the direct relationship between erosion and $T_d$. The influence upon erosion (Fig. 4) is not very significant; a decrease in $T_d$ from 1000°–500°F would only decrease this loss by 10%.

The product $\rho_c C_c$ is the volumetric heat capacity of the char; it has a relatively small beneficial influence upon the duration of ablators. Its influence upon the erosion rate is significant (Fig. 4) because of its retarding effect on surface temperature during transient heating periods. The influence of the specific heat of the virgin material ($C_v$) on duration is modest, approximately 10% with erosion (for doubling of the variable) and 20% without erosion. Influence upon the erosion rate is not appreciable, since this variable has very little effect upon the surface temperature of the char layer.

A high value of specific heat of the gaseous decomposition products ($C_d$) is beneficial in the transpiration and the mass addition processes, both of which directly influence surface temperature. If endothermic gas-phase reactions occur during transpiration, an appropriate increase in the effective $C_d$ is employed in the analytical model.

Volatile weight fraction of the resin ($f_v$) enters into the same processes as the specific heat or decomposition gases, but as noted from Figs. 2–4, their effectiveness is slightly different. In the transpiration equation, the volatile fraction appears only as a product with the specific heat of decomposition gases, but in the mass addition equation it is a stronger variable, accounting for the slight difference in effectiveness.

The molecular weight of the products of decomposition ($M_d$) appears only in the mass addition equation and apparently does not influence either durability or erosion rate. Consequently, variations in $M_d$ which result from processing

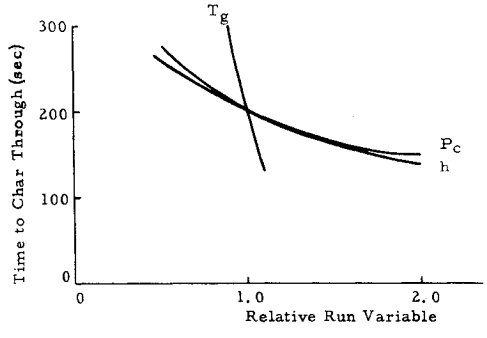


**Fig. 6 Time-to-char-through with run variable changes (with erosion).**

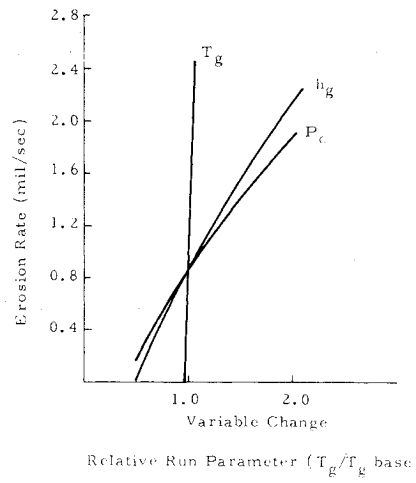


**Fig. 7 Run parameter influence on erosion.**

variations can be neglected, except for the inter-relationship that $M_d$ might have with $C_d$.

The thermal conductivity of the virgin material ($k_v$) has a negligible influence upon both duration and erosion rate because it is small; even if it were much higher, it still would provide no appreciable sink for the transferred heat. To investigate further, char depth and char rate were plotted against time for three ratios (0.5, 1, and 2) of $k_v$ to the reference value in Fig. 8. The higher $k_v$ material does char more slowly in the beginning, but at approximately 100 sec the rates cross over, and the higher-conductivity material chars more rapidly. The net result is a slight difference in time-to-char-through (3 in 270 sec). The time-to-char to depths less than the total thickness is more sensitive to $k_v$; the time-to-char to 0.2 in. varies by as much as 14 sec from an average value of 50 sec.

### Run Variables

The heat-transfer coefficient ($h$), in the absence of erosion, has only a minor influence on time-to-char-through (Fig. 5). This has also been shown by Lafazan.[6] When erosion occurs, however, the gas-film coefficient exerts a very strong influence upon the erosion rate (because of the sensitivity of the erosion equation with surface temperature) thereby influencing the time-to-char-through (Fig. 6). If $h$ can be halved, either by reducing $P_c$ or by some method of reducing heat rejection such as film cooling, then the erosion rate approaches zero. This then indicates the necessary design approach for conditions where erosion (e.g., at the throat) is intolerable. The design of divergent sections usually falls into the category of the nonerosive ablation because $h$ is very low for the supersonic exhaust gases.

Flame temperature is assumed to be the product of temperature and the square of $C^*$ efficiency; it strongly influences

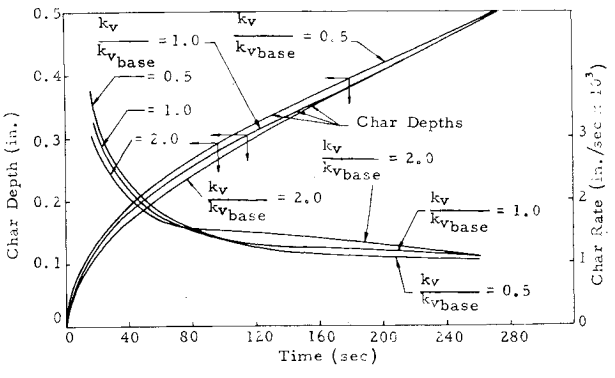


**Fig. 8 Char transients with virgin thermal conductivity influence.**

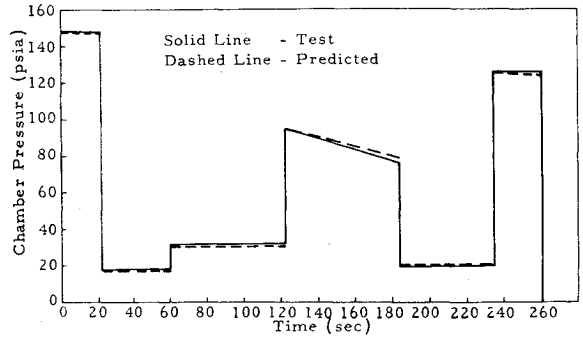


**Fig. 9 Duty cycle for engine *D*.**

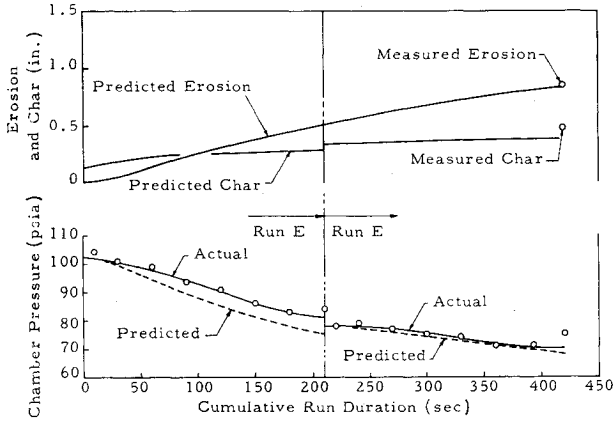


**Fig. 10 Throat plane data for engine *E*.**

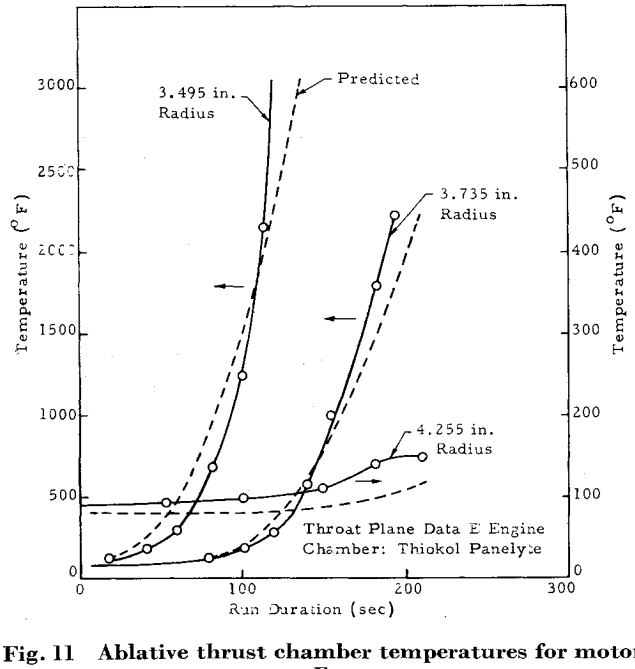


**Fig. 11 Ablative thrust chamber temperatures for motor *E*.**

time-to-char-through (Fig. 7) for both erosive and nonerosive ablation. A 1% change in durability and a 3% change with erosion result from a 1% change in flame temperature without erosion. This suggests that reductions in flame temperatures accomplished by reducing combustion efficiency or by mixture ratio shifts can be very effective in reducing both erosion rate and time-to-char-through.

**Table 2 Comparison of measured and calculated values for silica phenolic in 150-lb engines with $P_c$ = 150 psia[a]**

| | Engine | | |
|---|---|---|---|
| | *A* | *B* | *C* |
| $C^*$ efficiency | 94 | 96 | 100 |
| Duration, sec | 40 | 60 | 195 |
| Chamber region, in. | | | |
| Char depth (actual) | 0.24 | 0.32 | 0.55 |
| Char depth (calc.) | 0.23 | 0.30 | 0.46 |
| Erosion (actual) | 0 | 0 | 0 |
| Erosion (calc.) | 0 | 0 | 0 |
| Throat region, in. | | | |
| Char depth (actual) | 0.2 | 0.23 | ...[b] |
| Char depth (calc.) | 0.2 | 0.23 | ...[b] |
| Erosion (actual) | 0.12 | 0.17 | ...[b] |
| Erosion (calc.) | 0.13 | 0.186 | ...[b] |

[a] Propellants are $N_2O_4$ and 50% UDMH-50% $N_2H_4$; O/F = 2.
[b] Nonablative throat insert used in engine C.

## Comparison with Test Data

### Thrust Level Scaling

Table 2 compares measurements on sectioned thrust chambers and computed results for three 150-lb-thrust silica phenolic motors. The predicted and actual results are in good agreement. The listed char depth is the total depth accumulated due to both operation and heat soak after shutdown, and it is measured from the final surface. The thickness of virgin ablative consumed is the sum of the eroded and the char depths.

Table 3 compares test data and predicted results for two larger thrust engines with silica phenolic chambers. The *D* and *E* refer to different engines of the same configuration; Fig. 9 shows the duty cycle for *D*. The duty cycle for *E* consisted of two 200-sec runs, with complete cool-down between runs. The spread in predicted char depth for both engines ranges from 1 to 15% (see Table 3). The computed erosion losses are within 22% of the measured values. For motor *E*, Fig. 10 compares the predicted and measured values of char depth and erosion loss in the chamber pressure, and Fig. 11 compares computed and measured temperatures at

**Table 3 Effect of thrust level[a]**

| | Engine | |
|---|---|---|
| | RMD *D* | RMD *E* |
| Combustion performance, % | 96–99.8 | 99.8 |
| Duration, sec | 260 | 420 |
| Ablative | Silica phenolic | Silica phenolic |
| Mixture ratio | 2.1 | 1.8 |
| Chamber region (injector), in. | | |
| Char Depth (actual) | 0.30 | 0.64 |
| Char depth (calc.) | 0.34 | 0.65 |
| Erosion (actual) | 0 | 0 |
| Erosion (calc.) | 0 | 0 |
| Chamber region (nozzle end), in. | | |
| Char depth (actual) | 0.40 | 0.56 |
| Char depth (calc.) | 0.46 | 0.54 |
| Erosion (actual) | 0.06 | 0.44 |
| Erosion (calc.) | 0.061 | 0.41 |
| Throat region, in. | | |
| Char depth (actual) | 0.50 | 0.48 |
| Char depth (calc.) | 0.48 | 0.427 |
| Erosion (actual) | 0.33 (max) | 0.84 |
| Erosion (calc.) | 0.27 | 0.80 |

[a] Chamber pressure = 100 psia, thrust = 3000 lb, propellants are nitrogen tetroxide-50% UDMH-50% $N_2H_4$.

**Table 4 Effect of solid propellants[7] on silica epoxy throats**

| | |
|---|---|
| Thrust, lb | 7000 |
| Chamber pressure, psia | 610 |
| Propellant | Solid |
| Gas temperature, °F | 5800 |
| Duration, sec | 24 |
| Char depth (actual), in. | 0.16 |
| Char depth (calc.), in. | 0.135 |
| Erosion loss (actual), in. | 0.43 |
| Erosion loss (calc.), in. | 0.416 |

**Table 5 Effect of liquid propellants[8] on silica phenolic throats**

| | Engine | |
|---|---|---|
| | RMD *F* | Naval Ordnance Test Station[8] |
| Chamber pressure, psia | 150 | 300 |
| Propellants | $OF_2$-$B_2H_6$ | $CLF_3$-$N_2H_4$ |
| Duration, sec | 10 | 20 |
| Combustion performance | 99% | 98% |
| Char depth (actual), in. | 0.10 | 0.12 |
| Char depth (calc.), in. | 0.09 | 0.083 |
| Erosion (actual), in. | 0.12 | 0.34 |
| Erosion (calc.), in. | 0.142 | 0.36 |

three locations in the throat of the *E* motor. In view of the very steep temperature transients and gradients occurring in these low-conductivity materials, the time to attain any selected temperature is probably the best comparison criterion. The measured curves differ by less than 20 sec from the predicted curves at any temperature. The outermost thermocouple shows larger differences, but they occur at very low temperatures (below 150°), which are of less interest.

Considerable ablation data are available from solid propellant motors. The ability to use this ablation data for predicting the behavior of materials not previously used in liquid propellant engines would be extremely valuable (the converse is also true). Table 4 and Fig. 12 compare the predicted and measured results for a silica epoxy material used in the throat of a solid propellant motor.[7] The erosion constants for the predictions were established at Thiokol-RMD with a liquid motor using nitrogen tetroxide and hydrazine mixture at $P_c$ = 160 psia. These comparisons indicate that the accuracy is adequate for engineering purposes, even in the presence of alumina particles.

### Propellant Scaling

Another valuable design capability is that of predicting erosion, char, and temperature distributions for different propellant combinations. This has been demonstrated with this model by using the erosion rate constants for silica phenolic from motor firings using $N_2O_4$ and the hydrazine mix to predict results for $OF_2$-$B_2H_6$ and for $CLF_3$-$N_2H_4$ (Table 5). The results are indeed adequate for design purposes with different propellants.

## Conclusions

Results of this study have shown that analytical techniques can be used to predict quantitatively the ablative behavior of engineering materials. The thermal conductivity of the char layer and the density of the virgin material appear to be the strongest property variables affecting ablative performance. Doubling the thermal conductivity halves erosion; halving the thermal conductivity increases chamber durability (as defined by time-to-char-through) by a factor of 2. Doubling the virgin material density doubles both erosion resistance and time-to-char-through. More moderate improvements in ablative performance result from increases in the latent heat, decomposition temperature, and resin fraction of the ablative material.

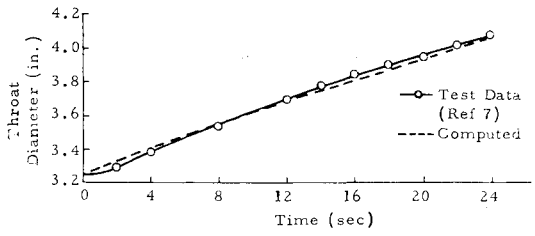


**Fig. 12 Erosion during solid propellant firing.**

Increasing the thickness of the ablative material improves chamber durability to a greater extent than increasing the material density. Thus, for a given duration, chamber weight can be minimized by using a large thickness of low-density material rather than a small thickness of high-density material. Increases in flame temperature and chamber pressure have much greater effects on performance of ablators than the thermal properties of the ablative material.

The often dichotomous results of a change in a material property (e.g., increasing char thermal conductivity increases erosion resistance but reduces time-to-char-through) indicate that ablative chamber optimization is best accomplished by utilizing composite designs. Thus, material properties could be manipulated independently to meet specific requirements.

## References

[1] Dusinberre, G. M., *Heat Transfer Calculations by Finite Differences* (International Text Book Co., Scranton, Pa., 1961).

[2] Hildalgo, H., "Theory of ablation of glassy materials for laminar and turbulent heating," Avco Research Rept. 62 (June 1959).

[3] Munson, T. R. and Spindler, R. J., "Transient thermal behavior of decomposing materials I.—General theory and application to convective heating," IAS Paper 62-30 (January 1962).

[4] McFarland, B., Joerg, P., and Taft, M., "Criteria for plastic ablation materials as a function of environmental parameters," Wright Air Development Div., Aeronautical Systems Div. TR 61-439 (May 1962).

[5] Jakob, M., *Heat Transfer* (John Wiley and Sons, Inc., New York, 1944), Vol. 1, p. 68.

[6] Lafazan, S., "Ablative thrust chambers for space applications," American Institute of Chemical Engineers, Preprint 5 (February 5, 1962).

[7] Hoetcher, H. E. and Mitchel, B. J., "Ablative nozzle concept, test results and scaling law," Avco Corp. Research and Development Div. (March 1962).

[8] Dettling, R. F., Naval Ordnance Test Station, letter to M. Luperi, Reaction Motors Div., Thiokol Chemical Corp. (December 1962).